

Spreading sequences for fast switching process in spin-valve nanopillars

Mario Carpentieri,¹ Marco Ricci,^{2,a)} Pietro Burrascano,² and Luis Torres³

¹DEIS, University of Calabria, I-87036 Rende (CS), Italy

²Polo Scientifico Didattico di Terni, University of Perugia, I-5100 Terni, Italy

³Department of Fisica Aplicada, University of Salamanca, E-37008 Salamanca, Spain

(Received 3 February 2011; accepted 2 March 2011; published online 22 March 2011)

A detailed study of the effects of binary spreading sequences (BSS) excitation in the magnetization dynamics of exchange-biased spin-valves driven by spin-transfer-torque has been carried out by full micromagnetic modeling. We show that the use of BSS allows to trigger the magnetization reversal by exciting its main precession modes. We compared our numerical results with the experimental ones reported by [Cui *et al.*, Phys. Rev. B **77**, 214440 (2008)], attaining quantitative agreement. Advantages of BSS as microwave source with respect to a sinusoidal signal are also reported and discussed. © 2011 American Institute of Physics. [doi:10.1063/1.3569947]

Spin transfer-driven magnetic switching may reduce the current densities required to induce switching or may increase the switching speed in magnetic random access memory nanopillars.^{1,2} The basic phenomena arise when a current flows through two nanomagnets—one acting as polarizer layer (PL), the other as free layer (FL) separated by a normal metal spacer or a thin insulator, as predicted by Slonczewski and Berger.³ For data storage applications, spin-transfer-torque-devices have to satisfy two main features: (i) reduce the critical current for compatibility with the complementary metal-oxide semiconductor technology and (ii) high thermal stability. Reductions in the critical current have been obtained by following different strategies.^{4–6} Among them, resonant switching-based memory architectures can be a key solution:⁷ switching processes assisted by a secondary sinusoidal source have been applied to different structures with several magnetic parameters and geometries.^{8,9} To be effective, the frequency value f_s of the sinusoidal excitation usually coincides to the free-precessional frequency f_P of the sample. Since nonlinear phenomena are present, in general f_P can be quite different from the ferromagnetic resonance (f_{FMR}) one, and it depends on both magnetic and geometric parameters.⁷ Studies about resonant switching have been also experimentally carried out by Cui *et al.*:⁸ they show that if a small sinusoidal “secondary” current pulse precedes the dc spin-polarized current, the switching probability, henceforth denoted as $P_{\uparrow\downarrow}$, can be enhanced and the switching time contextually decreases by properly choosing the frequency and the phase of the sinusoidal current. In this letter, we propose an innovative way to excite the magnetization able to trigger the reversal mechanism: such method exploits the peculiar spectral properties of the so-called binary spreading sequences (BSS) (Ref. 10) that allow to avoid the fine tuning of both frequency and phase of the secondary excitation. BSS are deterministic codes of finite length L , having randomness properties similar to white noise. In the last decades they have been extensively studied in communication theory and applied in several fields.¹¹ The main statistical properties of such sequences are summarized by their cyclic autocorrelation and cross-correlation functions:¹² in particular BSS combine a quite flat spectrum with a constant delivered

power. Two main families of BSS can be identified: the pseudonoise codes generated by a linear feedback shift register¹² and the Chaos-based BSS, that are inherently nonlinear ones.¹³ Linear BSS codes exist only for sequence length values, $L=2^n-1$, with n integer. On the other hand, Chaotic-based BSS do not exhibit length constraints but are suboptimal in the autocorrelation perspective.¹³ The use of Chaos-based BSS has allowed us to easily study the response of the nanopillars structures by smoothly varying the band of the excitation signal. Chaos-based BSS are attained by quantization of trajectories generated by a chaotic map $\mathcal{M}(\cdot)$ given a starting point x_0 : $\{\mathcal{T}(k, x_0): x_{k+1}=\mathcal{M}(x_k), \text{ for } k > 1\}$. By definition a map is chaotic when the resulting trajectory exhibits an aperiodic steady-state behavior that is not an equilibrium point, a periodic motion, or a quasiperiodic motion. A main trait of chaotic maps is their supersensitivity even to small changes in the initial condition, i.e., given two close values $x_0, x'_0=x_0+\delta x$, the resulting trajectories $\mathcal{T}(k, x_0), \mathcal{T}(k, x'_0)$ will be pretty uncorrelated after a few iterations. A comprehensive discussion about chaotic map theory lies outside the aim of this paper. The reader can find a detailed explanation in.¹³ For our purposes, it is sufficient to introduce how we have generated the BSS here adopted. We have chosen the logistic map $\{\mathcal{M}: x \in [0, 1] \mapsto [0, 1], x_0 \in [0, 1], x_{k+1}=\lambda x_k(1-x_k)\}$ with $\lambda \in (3.996, 4]$ and we defined a BSS of length L as $\{\text{BSS}[n]=Q\{x_n\}, n \in [0, L-1]\}$, being $Q\{\cdot\}$ a simple threshold quantization map

$$\text{BSS}[n] = Q\{x_n\} = \begin{cases} 1 & \text{if } x_n > \mu \\ -1 & \text{otherwise} \end{cases},$$

where the threshold parameter μ is the mean value of $\mathcal{T}(n)$. To render such BSS in analog signals we define the function: $\Psi_{\text{BSS}}(t, t_0, T, L) = \sum_{n=0}^{L-1} \text{BSS}[n](\theta_{t_0+(nT/L)} - \theta_{t_0+((n+1)T/L)})$ where t_0 is the starting time of the waveform, T is the overall signal duration, L is the length of the related BSS and $\theta_\tau = \theta(t - \tau)$. The bandwidth BW of $\Psi_{\text{BSS}}(t, t_0, T, L)$ increases linearly with L and it can be expressed as: $BW(T, L) = (L/2T) = (f_{\text{max}}/2)$. Of course different maps can be used, we chose the logistic map since it represents an archetypal example of how chaotic behavior arises from simple nonlinear dynamics.¹⁴

We want to show that the adoption of a broadband signal can optimally replace the use of a sinusoidal secondary ex-

^{a)}Electronic mail: marco.ricci@unipg.it.

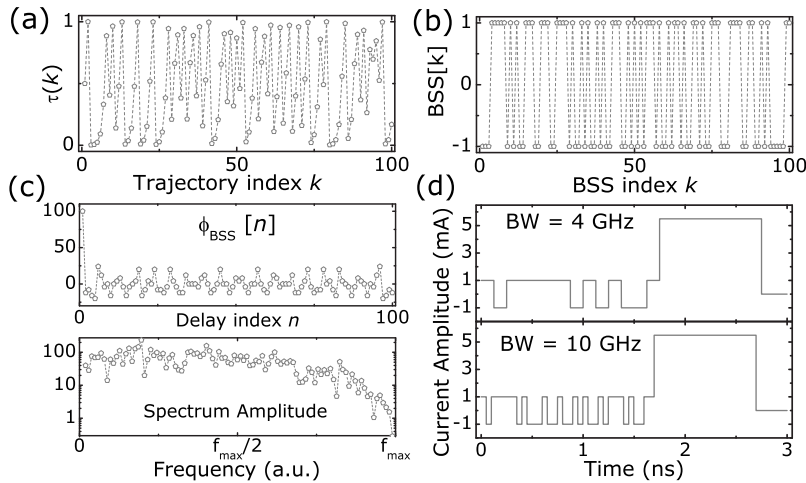


FIG. 1. (a) A trajectory $\mathcal{T}(k, 0.5)$ from logistic map with $\lambda = 3.998$; (b) the resulting BSS[k]; (c) auto-correlation function of BSS[k] (top) and spectrum amplitude for the corresponding $\Psi_{\text{BSS}}(t, t_0 = 0, T, L = 100)$; and (d) current waveforms for BSS secondary current with $BW = 4$ GHz and 10 GHz, respectively.

citation in stimulating the magnetization reversal of spin-valve nanopillars. We have therefore performed micromagnetic simulations adopting for the current the expression $\vec{i}(t) = \vec{i}_P(t) + \vec{i}_S(t)$ where $\vec{i}_P(t) = \hat{z}I_0(\theta_{T_1} - \theta_{T_1+T_2})$ represents the standard dc current pulse and $\vec{i}_S(t) = \hat{z}I_S\Psi_{\text{BSS}}(t, t_0 = 0 \text{ ns}, T_1, L)$ is the secondary excitation. Figure 1 shows two typical current waveforms used in numerical simulations and summarizes the main properties of the BSS. BSS excitation has been then tested on the experimental structure described in Ref. 8: an exchange-biased spin valve nanopillars composed by IrMn(8 nm), “Permalloy”Py(4 nm) [PL]/Cu(8 nm)/Py(4 nm)[FL] with elliptical cross sectional area ($150 \times 80 \text{ nm}^2$). We performed micromagnetic simulations based on the numerical solution of the Landau–Lifshitz–Gilbert–Slonczweski equation,³ where we have taken into account the standard effective field, the magnetostatic field due to the PL, and the Oersted field due to the current.¹⁵ As a starting point of our investigations we have reproduced the results attained by Cui *et al.*⁸ and, once retrieved, we carried out numerical simulations exploiting BSS as secondary excitation. For the sake of clarity we adopted the same parameter values used in Ref 8: effective exchange bias on the PL is 100 mT at 20 K and exchange bias field is at 45° from the elliptical easy axis. Moreover for all the switching simulations, we applied a bias field of 17 mT at 45° in order to compensate the magnetostatic coupling with the PL. The FL has been discretized in computational cells of $5 \times 5 \times 4 \text{ nm}^3$. The time step used was 32 fs and the current density is considered positive when the electrons flow from PL to FL. The thermal fluctuations have been taken into account as an additive stochastic contribution to the deterministic effective field for each computational cell.¹⁶ We first characterized the switching process with no microwave excitation: we found that at $T = 0 \text{ K}$, the critical current density needed to obtain the parallel to antiparallel transition of the magnetization within 10 ns was $J_0 = 2.9 \times 10^7 \text{ A/cm}^2$. This value was in quantitative agreement with the experimental one extrapolated by Cui *et al.*,⁸ $I_0 = (3.2 \pm 0.2) \text{ mA}$, considering the cross section area $A = 1.02 \times 10^{-14} \text{ m}^2$. Then we verified the influence of the thermal field on the switching processes by performing 50 iterations to find the value of $P_{\uparrow\downarrow}$ at the same critical current J_0 : we found that thermal effects do not trigger the process. We also noted that lower switching currents are obtained at lower temperatures, in agreement with the experimental work in Ref. 17. To complete this preliminary

analysis, we performed simulations to test rf-assisted switching at $T = 20$ and 300 K by setting the dc current at $J = 2.8 \times 10^7 \text{ A/cm}^2 < J_0$ and by applying a secondary sinusoidal field with frequency ranging from 0 to 15 GHz. At those values no reversal magnetization without thermal contribution occurred, whereas at $T = 300 \text{ K}$ we attained $P_{\uparrow\downarrow} = 2\%$. Micromagnetics results of the rf field effect show also that the optimal frequency in terms of $P_{\uparrow\downarrow}$ was 4 GHz. Figure 2(a) shows the frequency spectrum with (inset) the main excited modes computed by means of micromagnetic spectral mapping technique,¹⁸ where it is visible that at 4 GHz in the left and right part of the structure there are two main precessional regions whereas at 9 GHz there is only one region on the right side of the structure. On this basis, we studied the magnetization switching process under the application of chaos-based BSS secondary current excitation. We first analyzed the trend of $P_{\uparrow\downarrow}$ by varying the BSS bandwidth BW . The data achieved for $T = 20$ and 300 K are depicted in Fig. 2(b) together with the values of $P_{\uparrow\downarrow}^0$ attained by only adopting dc pulse current (i.e., $I_S = 0 \text{ mA}$).

These results can be compared with the ones reported in Ref. 8. In that case the enhancement of $P_{\uparrow\downarrow}$ due to the use of a secondary excitation was strongly dependent on both the frequency and the phase of the ac current: at the optimal frequency $f^* = 4.9 \text{ GHz}$, $P_{\uparrow\downarrow}$ varies from about 90% to 0% for a phase variation of 180° . Furthermore the optimal phase, 50° , seems to depend on several parameters, making not

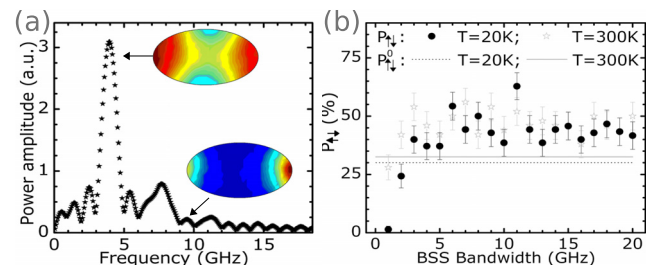


FIG. 2. (Color online) (a) Computed fast-Fourier-transform of the temporal evolution of the magnetization during the preswitching time (0–3 ns) by using micromagnetic spectral mapping technique. Inside panel: main excited precessional regions of the spatial distribution of the magnetization for $f_{\text{field}} = f_P = 4 \text{ GHz}$ and at greater frequency (9 GHz); (b) $P_{\uparrow\downarrow}$ vs BW for $M = 70$ iterations at $T = 20 \text{ K}$ (black circle) and at $T = 300 \text{ K}$ (open stars) by adopting the following values of the parameters (see Ref. 8): $I_S = 1.4 \text{ mA}$, $I_0 = 7.7 \text{ mA}$, $T_1 = 1.7 \text{ ns}$, and $T_2 = 1 \text{ ns}$. The horizontal lines represent the values of $P_{\uparrow\downarrow}^0$ at $T = 20$ and 300 K. Error bar indicates the percentage of error computed by means of binomial distribution.

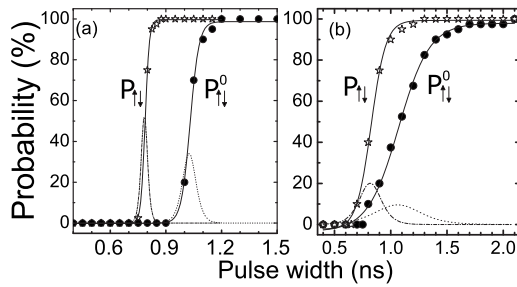


FIG. 3. $P_{\uparrow\downarrow}$ and $P_{\uparrow\downarrow}^0$ vs T_2 for $I_S \approx 1.5$ mA and $I_0 \approx 8.5$ mA together with a Boltzmann fitting (solid line) at (a) $T=20$ K and (b) $T=300$ K. Dashed-dotted and dotted lines represent the distributions of switching pulse duration, corresponding to $\partial P_{\uparrow\downarrow}/\partial T_2$ and $\partial P_{\uparrow\downarrow}^0/\partial T_2$, respectively.

trivial to find it with accuracy and making not effective the practical implementation of this method. On the other hand, in the case of BSS excitation we attained $P_{\uparrow\downarrow} < P_{\uparrow\downarrow}^0$ for $BW < f_p$, whereas for $BW > f_p$ we achieved a quite regular and constant trend at both temperature $T=20$ and 300 K with $P_{\uparrow\downarrow} \approx 45\% > P_{\uparrow\downarrow}^0$. This means that by using a BSS with $BW \gg f_p$, $P_{\uparrow\downarrow}$ does not depend from the particular sequences adopted.

Cui *et al.*⁸ also experimentally demonstrated that the secondary current can lead to a relevant speed-up of the switching time. We compare their results with the outcomes of our micromagnetic simulation in which sinusoidal secondary current is replaced by BSS signal. Figure 3 shows $P_{\uparrow\downarrow}$ versus T_2 at $T=20$ and 300 K. As expected $P_{\uparrow\downarrow}$ increases with T_2 in both cases [see Figs. 3(a) and 3(b)] and the transition from $P_{\uparrow\downarrow}=0\%$ to $P_{\uparrow\downarrow}=100\%$ is much more soft at $T=300$ K due to thermal effects. Comparing these data with those shown in Fig. 4 of Ref. 10, we observe that the use of BSS signal assures a much more deterministic behavior of the switching process. In fact, by adopting rf secondary excitation the transition of $P_{\uparrow\downarrow}=0 \rightarrow 100\%$ at $T=300$ K is attained for a variation in T_2 equal to $\Delta T_2 = 1.2$ ns (see Fig. 4 of Ref. 8), and the use of rf signal before square-pulse does not trigger the process. On the other hand, by adopting the BSS this transition time is reduced to $\Delta T_2 \approx 0.6$ ns. Much more evident is the effect at low temperature. At $T=20$ K the transition $P_{\uparrow\downarrow}=0 \rightarrow 100\%$ is achieved for $\Delta T_2 = 0.1$ ns with BSS and for $\Delta T_2 \approx 3$ ns considering rf source, giving a very deterministic behavior of the magnetization during the switching process. Autocorrelation properties of BSS imply that the frequency bandwidth of the sequences is wide exhibiting a quite flat spectrum and exciting all the frequencies including the typical one of the free magnetization precession. Furthermore, peculiar properties of BSS give a characteristic phase of the combined signal that the switching probability is more deterministic and it is not strongly dependent as in the case of a secondary sinusoidal source.

In summary, we propose a way to obtain fast switching and reduced current density in exchange-biased spin-valve nanopillars. The validation of the proposed technique was carried out by means of micromagnetic computations and by comparing our results with the ones attained by Cui *et al.*⁸ With respect to traditional rf assisted switching, the use of chaos-based BSS allows to overpass two critical points present when a sinusoidal “secondary” excitation is considered. If the rf frequency was different from the free-precession frequency of the magnetization, f_p , the reversal process is not triggered by the rf source. Since f_p differs

from f_{FMR} , usually it is difficult to find its right value. Moreover the method to trigger switching process found by Cui *et al.*⁸ based on the use of a rf pulse combined with a square-pulse demonstrated that the switching process was strongly dependent not only of the rf frequency but also of the phase. From a practical point of view, the determination of the best phase is not trivial. We found that using BSS signal in combination with a large square-pulse, the switching probability is not dependent from frequency and phase of the rf signal and at both low and room temperatures the switching process is much more deterministic than using rf sinusoidal signal. We stress that to improve the statistical significance of the simulations, in all the experiments carried out adopting BSS we employed a different sequence for each iteration, i.e., a different x_0 . Thus the results come out from an average performed with respect to thermal fluctuations and to spectral properties of different realizations of BSS. A methodical optimization of BSS can further improve $P_{\uparrow\downarrow}$; this aspect lies outside the aim of the present work and will be tackled in a further work.

The authors thank Sergio Greco for his support. This work was supported by Fondazione Cassa di Risparmio di Terni e Narni and by Spanish Projects under Contract Nos. MAT2008-04706/NAN and SA025A08.

- ¹S. I. Kiselev, J. C. Sankey, I. N. Krivorotov, N. C. Emley, R. J. Schoelkopf, R. A. Buhrman, and D. C. Ralph, *Nature (London)* **425**, 380 (2003).
- ²I. N. Krivorotov, N. C. Emley, J. C. Sankey, S. I. Kiselev, D. C. Ralph, and R. A. Buhrman, *Science* **307**, 228 (2005).
- ³J. C. Slonczewski, *J. Magn. Magn. Mater.* **159**, L1 (1996); **195**, 261 (1999); **247**, 324 (2002); L. Berger, *Phys. Rev. B* **54**, 9353 (1996).
- ⁴O. Ozatay, N. C. Emley, P. M. Braganca, A. G. F. Garcia, G. D. Fuchs, I. N. Krivorotov, R. A. Buhrman, and D. C. Ralph, *Appl. Phys. Lett.* **88**, 202502 (2006).
- ⁵G. Finocchio, O. Ozatay, L. Torres, M. Carpentieri, G. Consolo, and B. Azzzerboni, *IEEE Trans. Magn.* **43**, 2938 (2007).
- ⁶P. M. Braganca, O. Ozatay, A. G. F. Garcia, O. J. Lee, D. C. Ralph, and R. A. Buhrman, *Phys. Rev. B* **77**, 144423 (2008).
- ⁷M. Carpentieri, G. Finocchio, B. Azzzerboni, and L. Torres, *Phys. Rev. B* **82**, 094434 (2010).
- ⁸Y.-T. Cui, J. C. Sankey, C. Wang, K. V. Thadani, Z.-P. Li, R. A. Buhrman, and D. C. Ralph, *Phys. Rev. B* **77**, 214440 (2008).
- ⁹S. H. Florez, J. A. Katine, M. Carey, L. Folks, O. Ozatay, and B. D. Terris, *Phys. Rev. B* **78**, 184403 (2008).
- ¹⁰R. L. Peterson, D. E. Borth, and R. E. Ziemer, *An Introduction to Spread-Spectrum Communications* (Prentice-Hall, Upper Saddle River, 1995).
- ¹¹P. Burrascano, M. Carpentieri, A. Pirani, and M. Ricci, *Meas. Sci. Technol.* **17**, 2973 (2007); S. W. Golomb and G. Gong, *Signal Design for Good Correlation: For Wireless Communication Cryptography, and Radar* (Cambridge University Press, New York, 2005).
- ¹²S. Golomb, *Shift Register Sequences* (Holden-Day, San Francisco, 1967); D. V. Sarwate and M. B. Pursley, *Proc. IEEE* **68**, 593 (1980).
- ¹³G. Mazzini, G. Setti, and R. Rovatti, *IEEE Trans. Circuits Syst., I: Regul. Pap.* **44**, 937 (1997); *Electron. Lett.* **35**, 1054 (1999).
- ¹⁴H. G. Schuster and W. Just, *Deterministic Chaos. An Introduction*, 4th ed. (Wiley, Weinheim, 2005).
- ¹⁵M. Carpentieri, L. Torres, B. Azzzerboni, G. Finocchio, G. Consolo, and L. Lopez-Diaz, *J. Magn. Magn. Mater.* **316**, 488 (2007); A. Romeo, G. Finocchio, M. Carpentieri, L. Torres, G. Consolo, and B. Azzzerboni, *Physica B* **403**, 464 (2008).
- ¹⁶W. F. Brown, *Phys. Rev.* **130**, 1677 (1963); D. M. Apalkov and P. B. Visscher, *Phys. Rev. B* **72**, 180405(R) (2005); G. Finocchio, V. S. Pribyag, L. Torres, R. A. Buhrman, and B. Azzzerboni, *Appl. Phys. Lett.* **96**, 102508 (2010).
- ¹⁷A. A. Tulapurkar, T. Devolder, K. Yagami, P. Crozat, C. Chappert, A. Fukushima, and Y. Suzuki, *Appl. Phys. Lett.* **85**, 5358 (2004).
- ¹⁸L. Torres, L. Lopez-Diaz, E. Martinez, G. Finocchio, M. Carpentieri, and B. Azzzerboni, *J. Appl. Phys.* **101**, 053914 (2007).